Morphodynamics of a growing microbial colony driven by cell death

Pushpita Ghosh and Herbert Levine

Phys. Rev. E **96**, 052404 — Published 8 November 2017

DOI: 10.1103/PhysRevE.96.052404

Morphodynamics of a growing microbial colony driven by cell-death

Pushpita Ghosh[1*] and Herbert Levine[2,3]
[1] *Centre for Interdisciplinary Sciences, Tata Institute of Fundamental Research, Hyderabad 500107, India*
[2] *Center for Theoretical Biological Physics, Rice University, Texas 77005, USA and*
[3] *Department of Bioengineering, Rice University, Texas 77005, USA.*

Bacterial cells can often self-organize into multicellular structures with complex spatiotemporal morphology. In this work, we study the spatiotemporal dynamics of a growing microbial colony in the presence of cell-death. We present an individual-based model of non-motile bacterial cells which grow and proliferate by consuming diffusing nutrients on a semi-solid two-dimensional surface. The colony spreads by growth forces and sliding motility of cells and undergoes cell-death followed by subsequent disintegration of the dead cells in the medium. We model cell-death by considering two possible situations: in one of the cases, cell-death occurs in response to the limitation of local nutrient, while the other case corresponds to an active death process, known as apoptotic or programmed cell-death. We demonstrate how the colony morphology is influenced by the presence of cell-death. Our results show that cell-death facilitates transitions from roughly circular to highly branched structures at the periphery of an expanding colony. Interestingly, our results also reveal that for the colonies which are growing in higher initial nutrient concentrations, cell-death occurs much earlier compared to the colonies which are growing in lower initial nutrient concentrations. This work provides new insights into the branched patterning of growing bacterial colonies as a consequence of complex interplay among the biochemical and mechanical effects.

I. INTRODUCTION

Microbial colonies are the most widely studied multicellular organizations in the realm of living matter. From an individual cell or a small cellular aggregate, a complex multicellular spatial structure can develop. In some cases this structure is commonly known as biofilm in which bacterial cells adhere to each other while being embedded in a self-secreted extracellular matrix [1–4]. An expanding microbial colony is influenced by a number of processes including cellular growth-division, surface attachment-detachment, motility, secretion of extracellular polymeric substances, mechanical, chemical and hydrodynamic interactions [5–19]. Moreover, microbial communities very often encounter unfavorable conditions around their natural environment, such as nutrient limitation, presence of competitors and harmful chemicals during antibiotic treatment [20–23].

One of the characteristic processes associated with a developing multicellular organization is cell death [2, 4, 20, 22, 24–27] which is one of the least understood among the aforementioned processes. Different forms of cell-death in bacteria have been reported in previous studies [20–22, 27, 28]. It has been shown that B. *subtilis* delays sporulation by killing and thereby supplying food for their non-sporulating siblings to prevent unnecessary spore formation [20, 22, 29–31]. Recent experimental studies have emphasized the role of heterogeneous cell-death on spatial morphology in a B. *subtilis* biofilm [4, 14].

More generally, in a bacterial population, responding to adverse conditions, cells can regulate the death-program for the benefit of the overall colony. Programmed cell-death(PCD) is one such process, defined as an active mechanism that results in cell suicide [21, 22, 32–34]. It has been reported that upon amino-acid starvation, E. *coli* undergoes programmed altruistic death, during which the dying cells provide nutrients for the survival of other cells [35, 36]. In Refs [37, 38], the presence of significant amounts of extracellular DNA within P. *aeruginosa* biofilm provides strong evidence of PCD and lysis of the dead cells during biofilm formation. Overall, the understanding of the underlying causes, mechanisms, and subsequent role of various cell-death processes remains largely unexplored.

Depending upon the particular bacterial species and environmental conditions, a wide variety of morphological patterns can emerge. For instance, B. *subtilis* exhibits different types of patterns, ranging from disk-like colonies to dense or sparse branched morphology, including diffusion-limited aggregation-like patterns, compact Eden-like structures and concentric ring-like morphologies [39, 40]. Attempts have been made towards understanding the occurrence of different morphological instabilities and the concomitant pattern formation, both experimentally and theoretically. Earlier studies have revealed that discrete nature of bacteria and inherent fluctuations can be responsible for the diffusive instabilities leading to the roughening of expanding fronts in growing colonies [41, 42]. A cut-off based reaction-scheme was employed in those studies to explain such roughening. Moreover, Golding and co-workers has pointed out that the role of a death term in cut-off-based reaction-diffusion model, is to stabilize the branching instability[43]. However, a sophisticated model which automatically takes care of the discrete particle nature and the fluctuations and couples them to microbial growth dynamics is still elusive.

*Email Address: pghosh@tifrh.res.in

In this regard, the key questions that we want to explore in the present study are:
(i) *How and to what extent might nutrient depletion induced cell-death affect the growth and morphology of a developing colony?*
(ii) *What is the role of apoptotic/programmed cell-death and to what extent can it regulate the growth dynamics and morphology?*
(iii) *To what extent can the altruistic aspects of programmed cell-death affect the growth dynamics?*

The objective of the present study is to model cell-death in an expanding bacterial colony to gain an understanding of its influence on growth and morphological dynamics. To address these issues, we first use a cut-off based reaction-diffusion model including cell-death and lysis as a prelude. We observe branching instabilities at the colony front. In agreement with the previous works, the cut-off based reaction-term apparently includes at least qualitatively the effect of discreteness and fluctuations in the growing colony [41, 42]. However, the main focus of the present work is to construct an individual-based model which automatically takes care of discrete nature of bacterial cells and the resultant inherent fluctuations in the colony. We implement two possible rules for cell-death: (1) nutrient-limited cell-death: a cell dies if the local nutrient level goes below a certain value; (2) apoptotic or programmed cell-death (PCD): random active cell-death which means cells commit suicide in a random manner with a certain rate. Our study suggests that not only fluctuations are important but also cell-death is crucial to develop branching patterns in the colony front. We show that colony morphology depends upon the rate and pattern of cell-death. In particular, while nutrient limitation alone gives rise to a colony with a rough interface of live peripheral cells moving outwardly, adding death gives rise to an accumulation of dead and disintegrated cells in the interior of the growing colony which now can develop highly branched structures at the periphery. Moreover, we show that initial nutrient concentration plays an interesting role for the local nutrient competition and the initiation of cell-death. Our result predicts the emergence of branched morphology in a developing microbial colony mediated by cell-death which therefore appears to be a significant factor in the evolution of spatiotemporal order in bacterial colonies.

II. CUT-OFF BASED REACTION-DIFFUSION MODEL

We consider a mean-field type reaction-diffusion system governing non-motile bacteria grown on a semi-solid agar surface in presence of a diffusing nutrient. We begin with the Kessler-Levine equations [41]:

$$\frac{\partial u}{\partial t} = uv\Theta(u-\epsilon) + D\nabla^2 u \tag{1}$$

$$\frac{\partial v}{\partial t} = -uv\Theta(u-\epsilon) + \nabla^2 v \tag{2}$$

where ϵ is the threshold density for growth, and Θ is the Heaviside step function(1 if $(u > \epsilon)$, 0 otherwise). The concentration of bacteria and nutrient/food are represented by u and v respectively. The food consumption term is of the form $f(u, v) = uv$, which is a widely used low-nutrient approximation and the parameter $D = 0.01$, represents the ratio of diffusivity of bacteria and nutrient. The cut-off in the reaction term at small bacteria density is used to represent the discreteness of bacteria and fluctuations present in a growing colony which are responsible for the existence of a diffusive instability [41, 42]. We carry out numerical simulations of the reaction-diffusion model (Eqns. 1-2) with zero-flux boundary condition by an Euler method for time-marching with a time step of 0.005, and standard finite-difference scheme in a square domain of length $L = 250$ with a grid size of 0.25, for resolving the diffusion. As an initial condition, we consider a small circular inoculation of bacteria with some randomness in its density at the center of the square box and the initial concentration of the nutrient field is kept equal throughout the box. As can be seen from the Figure-1 under a no-death condition, there arises a diffusive instability but deep branching does not occur since emergent dips are quickly healed. It has been suggested that one of the ways to obtain and stabilize the branch formation is to introduce a death term [43].

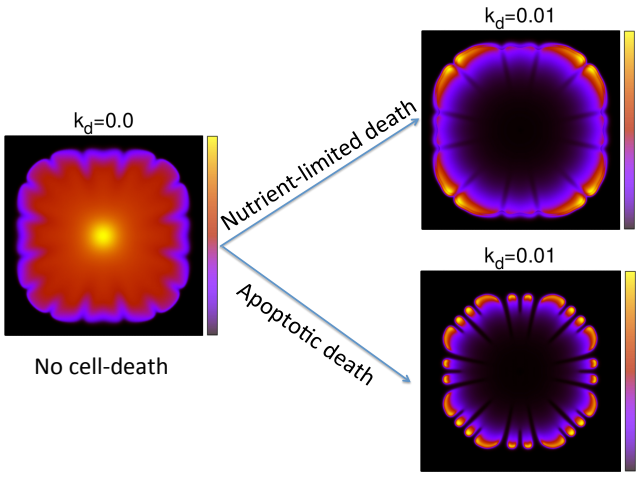

FIG. 1: (Color online) Snapshot of colonies (alive+dead) in absence and in presence of cell-death for a cut-off $\epsilon = 0.2$. For both the cases of nutrient-limited-death and apoptotic-death, value of the rate of cell-death is $k_d = 0.01$ and rate of lysis of the dead cells is $k_{lys} = 0.002$. Shown here is the snapshot of a simulated colony in case of nutrient-limited cell-death, which occurs when local nutrient concentration crosses a threshold value of $C_{thresh} = 0.001$. The color bar shows the variation of concentrations from low(blue) to high(yellow); black corresponds to a zero value.

To include the effect of cell-death and subsequent lysis,

we here consider a modified model as follows:

$$\frac{\partial u}{\partial t} = uv\Theta(u-\epsilon) - k_d u + D\nabla^2 u \quad (3)$$

$$\frac{\partial v}{\partial t} = -uv\Theta(u-\epsilon) + \nabla^2 v \quad (4)$$

$$\frac{\partial w}{\partial t} = k_d u - k_{lys} w \quad (5)$$

where k_d is the rate of cell-death which leads to the accumulation of dead and inactive population of bacteria represented by $w(x, y, t)$. These eventually disintegrate with time at a constant rate k_{lys}. We now carry out numerical simulations of the reaction-diffusion model (Eqns-3 to 5) following the aforementioned method for different values of the cell-death rate k_d, at a fixed rate of cell-lysis $k_{lys} = 0.002$. We observe enhanced branching patterns at the colony periphery upon increasing k_d, as can be seen from Figure-1. Specifically, under the condition of nutrient-dependent cell-death, we assume a threshold concentration of nutrients, $C_{thresh} = 0.001$ below which the cell starts to die. Therefore, we multiply the death term $k_d u$ of Eqns (3 and 5) by a function H such that ($H = 1$ for $v < C_{thresh}$, or $H = 0$ otherwise). For apoptotic death, cells die randomly from any part of the growing colony.

Apparently, cell-death seems to be a significant parameter in branch formation. However, it appears that in the absence of a cut-off term, cell-death can not by itself lead to such branching instabilities at colony fronts (result not shown). This suggests that discreteness and inherent fluctuations play crucial roles in causing cause front instabilities. Cell-death accompanies fluctuation-driven instability to create enhanced branching. The underlying reason here lies in the fact that bacteria left behind the propagating front become dead and inactive. They are unable to move to close the emerging dips, thus allowing deep branches to form.

Although the above cut-off based continuum model has been able to show branch formation, a more sophisticated methodology and a better model is a necessity to quantitatively account for the discrete particle nature and the inherent fluctuations in an expanding colony. In this regard, we use an individual-based/agent-based model of expanding microbial colony which by its very nature takes care of the discreteness of cells and inherent fluctuations present in a colony. In the following section, we will describe our individual-based model including the presence of cell-death.

III. THE INDIVIDUAL-BASED MODEL AND METHOD

Next, we consider colony dynamics by means of individual-based modeling [11, 15]. In our model, an individual bacterial cell is considered as a nonmotile growing spherocylinder having constant diameter ($d_0 = 1\mu m$) and variable length l. We consider a two dimensional semi-solid surface (300μm $\times$ 300μm)for colony growth and therefore each cell is represented by a spatial coordinate $r = (x, y)$ and unit vectors (u_x, u_y) representing the orientation of the symmetry axis of the cell. The growth of a cell depends on the availability of local nutrients which are diffusing in the medium. The two dimensional surface is discretized into equally-sized square units. Each square patch is characterized by a nutrient concentration $c(x, y)$. As the simulation of local nutrient competition between individual cells is one of the primary goals, the patch dimension is presumed to be in the same order of magnitude as the microbial cell size, more specifically $2\mu m$. The colony expands due to the utilization of local nutrient governed by a diffusion equation linked to a sink term which reflects the nutrient consumption by the cells,

$$\frac{\partial c}{\partial t} = D\left(\frac{\partial^2 c}{\partial x^2} + \frac{\partial^2 c}{\partial y^2}\right) - k\sum A_i f(c(x_i, y_i)), \quad (6)$$

where $A_i = \pi r_0^2 + 2r_0 l_i$ is the area of cell i, $r_0 = d_0/2$ is the radius of end-cap, l is the length of the cell and x_i, y_i is its spatial coordinates. Initially the nutrient concentration has been taken to be $c = C_0$ everywhere and c is kept constant at the edges of the simulation box, which is taken large enough to ensure that there is no direct effect of the boundaries. The nutrient is utilized by the bacterial cells at a rate $kf(c)$ per unit biomass density where $f(c)$ is a monotonically increasing dimensionless function. In our simulations, we assume $f(c) = c/(1+c)$, a Monod function with half-saturation constant equal to one (in arbitrary units).

In our model, a cell i, grows by elongation in accordance with the relation $dl_i/dt = \phi.(A_i/\bar{A}).f(c(x_i, y_i))$ where ϕ is the constant growth parameter and $\bar{A} = \pi r_0^2 + \frac{3}{2} r_0 l_{max}$ is the average area [11, 15] in a two-dimensional representation. This is equivalent to assuming that the cells grow at a rate proportional to the biomass or volume of a cell [44] and taking the volume to be simply a fixed height times the two-dimensional area. An alternative could be to compute the real 3D volume of an assumed spherocylinder which yields a slightly different formula; we expect that this change would make only very minor changes in our results. One consequence of including the cell-area A_i in the above relation is that, it ensures, that the colony grows at the same rate for cells with different average aspect ratios.

Once a cell reaches a critical length l_{max}, it splits at a rate k_{div} into two independent daughter cells with orientations roughly the same as the mother cell but with small randomness. This randomness in the orientation incorporates the effect of various irregularities in the system e. g., roughness of the agar surface, slight bending of the cells etc. This stochasticity allows for quasi-circular colony growth instead of cells growing as long filaments. We assume cells interact directly by mechanical interactions in accordance with the Hertzian theory of elastic contact [8, 10] by repelling neighboring cells in case of spatial overlap. The force between two spherocylinders

is approximated by the force between two spheres placed along the major axis of the rods at such positions that their distance is minimal [15]. If the shortest distance between the two spherocylinders is r and $h = d_0 - r$ is the overlap, then the force is assumed to be $F = Ed_0^{1/2}h^{3/2}$ where E parametrizes the strength of the repulsive interaction proportional to the elastic modulus of the cell. $E \longrightarrow \infty$ implies perfectly hard cells but in fact our simulation uses a finite value of E (see Table-I), allowing for some deformation. In addition to direct inter-cellular interaction there is competition for nutrient which can be considered as indirect interaction between microbial cells mediated by the environment. In such a dense system, inertia can be neglected and we consider the over-damped dynamics for the cellular motion. The equations of motion are given by

$$\dot{\mathbf{r}} = \frac{1}{\zeta l}\mathbf{F}, \tag{7}$$

$$\omega = \frac{12}{\zeta l^3}\tau \tag{8}$$

where ζ is the friction per unit length of cell and r and ω are position and the cells angular velocity respectively. The corresponding linear forces and torques are represented by F and τ.

Parameter	Symbol	Simulations
Maximum length	l_{max}	4.0μm
Diameter of cell	d_0	1.0μm
Linear growth rate	ϕ	$1.5\mu m\ hr^{-1}$
Cell-division rate	k_{div}	$0.2hr^{-1}$
Cell-death rate	k_d	$0.00075 - 0.005hr^{-1}$
Lysis rate of dead cells	k_{lys}	$1.0hr^{-1}$
Elastic modulus of alive cells	E	$3 \times 10^5 Pa$
Elastic modulus of dead cells	E_d	$10^4 Pa$
Friction coefficient	ζ	$200Pa.hr$
Initial nutrient concentration	C_0	$0.5fg\ \mu m^{-3}$
Nutrient consumption rate	k_c	$6.0hr^{-1}$
Diffusion rate of nutrient	D	$400\mu m^2 hr^{-1}$

TABLE I: Parameters and constants used in the simulations

We implement cell-death in a growing colony following two possible scenarios:
Method-1: nutrient-depletion mediated cell-death: In this case we assume that the nutrient level going below a certain threshold triggers cell-death. This assumes that when bacteria are starving they start dying in response, without making any active apoptotic decision.
Method-2: apoptotic or programmed-cell-death: In this approach we assume that some of the bacterial cells decide to undergo random death, quite similar to what happens in eukaryotic multicellular systems.

To explore the role of dead cells in governing colony dynamics, it is necessary to investigate both the mechanical properties and the effect of lysis of the dead cells. We typically consider the dead cells to have a low repulsive elastic coefficient as compared to that of alive cells. Furthermore, we assume that dead cell undergoes lysis following a shrinking of its size at a certain rate; eventually it will disintegrate completely and subsequently get removed from the colony. To understand the combined effect of weaker forces and lysis, we carry out several controlled variations on our simulations: (i) keeping the mechanical interactions the same as for alive cells as long as the dead cells have not yet completely disintegrated and been removed from the system, (ii) lowering the mechanical repulsive forces of dead cells but not allowing them to disintegrate, (iii) keeping the repulsive mechanical forces of dead cells the same as for alive cells but including the fact that dead cells undergo rapid lysis. These are discussed in the following section.

IV. RESULTS AND DISCUSSION

The main focus of the current study is to understand the role of cell-death determining the dynamics and morphology of a growing bacterial colony. We begin our study by simulating a few number ($N = 5$) of bacterial cells attached to a two-dimensional surface and explore how the colony develops. Microbial cells uptake local nutrient available in the medium in order to grow, divide and spread by mechanically-driven sliding motility. First, we ignore cell death. The colony expands from the center of the two-dimensional simulation box, leading to nutrient depletion in the interior region due to the increase in the local cell-density. As a result, the growth of the cells in the interior region becomes slower. We see that a roughly circular colony develops as shown in Movie-1 and also demonstrated in the snapshots in Figure-2 under no death condition.

Next, we implement cell-death considering the following two processes: nutrient-depletion-driven cell-death and apoptotic or programmed cell-death. For the process of *nutrient-depletion-driven cell-death*, we implement the possibility of nutrient-limited death after initial colony development up to time T=300 hr. When the local nutrient level falls below a certain threshold value, which we choose in the simulations as $C_{thresh} = 0.001fg/\ \mu m^3$, the starving cells cannot cope with the nutrient-deficient condition and start to die. As already mentioned that once cell-death occurs, the dead cells disintegrate at a fixed rate until they disappear from the colony. Movie-2 demonstrates the colony development in presence of nutrient-dependent-cell-death. The corresponding snapshots of simulated growing colony with respect to time are shown in Figure-2 under nutrient-limited death condition. We observe a roughly circular band of live cells, that grows outward, keeping the dead and disintegrated cells in the interior region since the nutrient comes from the edges of the simulation box. Moreover, we find that the spatiotemporal morphology at the colony edge undergoes a clear transition from roughly circular to a branched

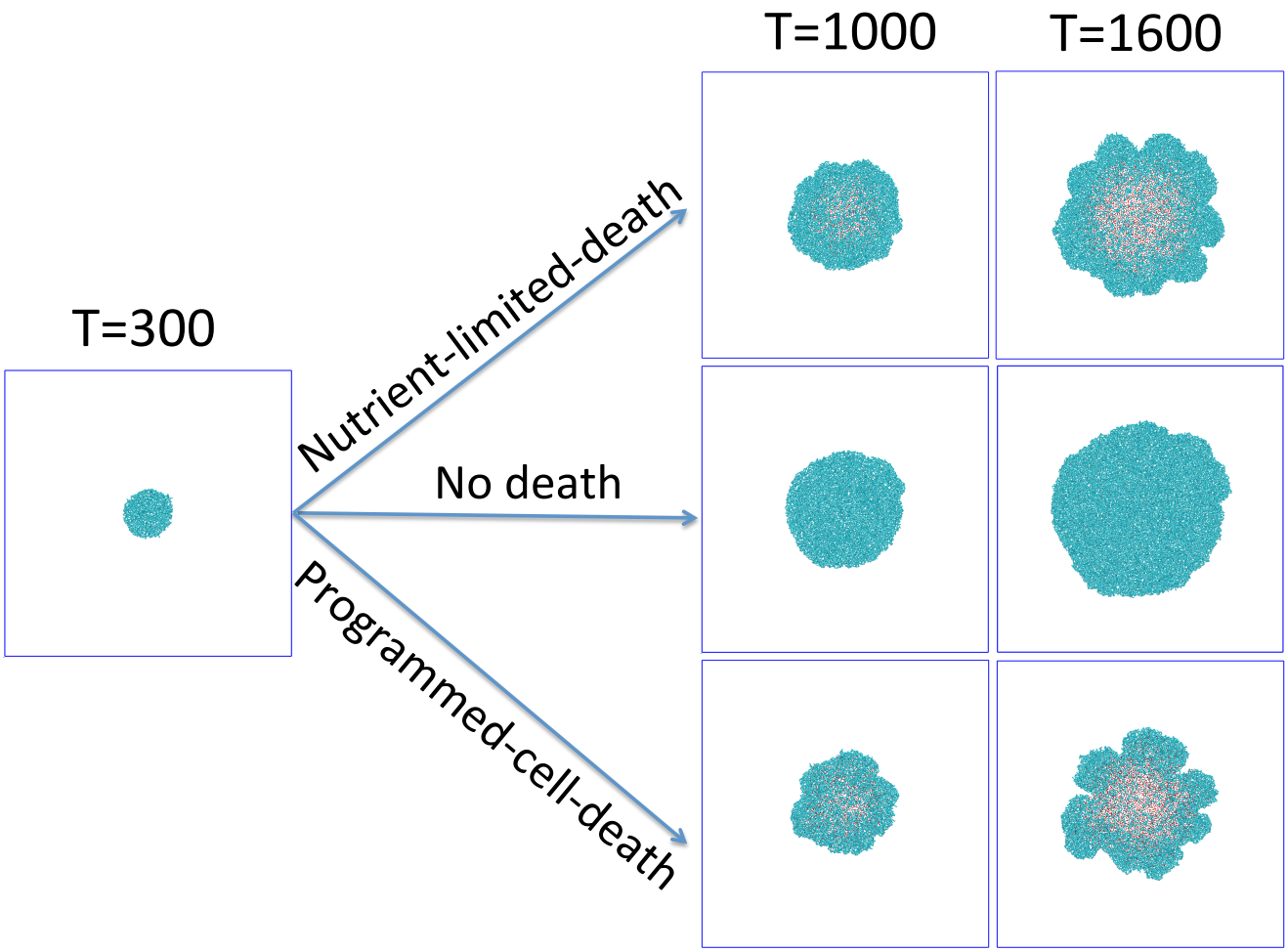

FIG. 2: (Color online) Spatiotemporal morphology of the growing colonies with respect to time in presence and absence of cell-death. For both the cases of nutrient-limited-death and programmed-cell-death, the rate of cell-death is $k_d = 0.001$. Shown here are the snapshots of a simulated colony which occurs for a threshold concentration of the local nutrient level $C_{thresh} = 0.001$ in the case of nutrient-limited cell-death. Programmed cell-death occurs randomly without any concentration threshold of the nutrient concentration. Here alive cells are represented by spherocylinders (cyan) and dead and disintegrated cells are depicted in the form of tiny red dots. All the other parameters are chosen to be same as given in the Table I.

structure as time progresses.

On the other hand, similar to what occurs in eukaryotic multicellular systems, *apoptotic or programmed cell-death* might occur in a multicellular bacterial populations. The underlying mechanism of apoptotic or PCD is different depending upon the type of stress involved in the particular microbial colony. Why and how bacteria switch on suicide program is poorly known. Our objective here is to predict the significance of programmed cell-death in a growing colony without specifying in detail any particular mechanism. To understand and compare the role of apoptotic or PCD in growing colony, we impose random cell-death with a fixed rate in our simulations after the colony grows to time T=300 hr. Movie-3 demonstrates the simulation result of a growing colony in presence of apoptotic death which is also elucidated in Figure-2 under the condition of programmed cell-death. PCD occurs randomly from any part of the colony irrespective of the local nutrient availability. As time goes on, in the colony center (mostly) the cells stop their growth and division, dead cells accumulate and the expanding front shows a transition from roughly circular to a highly branched morphology at the colony edge.

As we can observe the development of branched structures at the colony edges in presence of cell-death, it is useful to investigate in detail how the colony morphology depends upon the presence of cell-death. What are the characteristic properties that can imply the certain role of cell-death in a growing colony governing its morphological dynamics? To answer these questions, we now compute the time profile of effective radius of a growing colony and speed of colony-front in presence and absence of cell-death. The effective radius as time progresses as shown in Figure-3A, which reveals that colony spreading

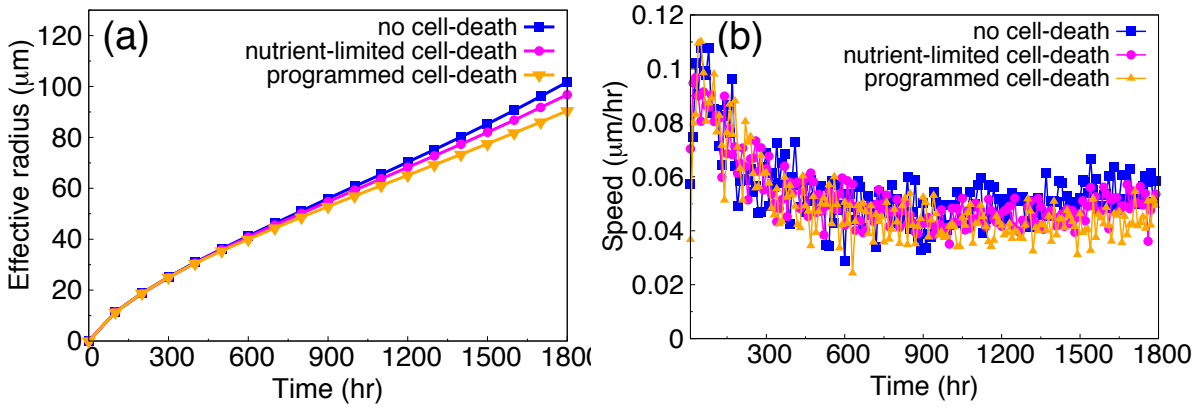

FIG. 3: (Color online) (A) Plot of effective radius of the growing colonies with respect to time. (B) Plot of the speed of the colony with respect to time. The blue curve (with filled squares) corresponds to no-death situation whereas the magenta (with filled circles) and orange (with filled triangles) curves correspond to nutrient-limited and programmed cell-death respectively. Rate of nutrient-limited and programmed cell-death is $k_d = 0.001$ and all the other parameters are same as given in the Table-1.

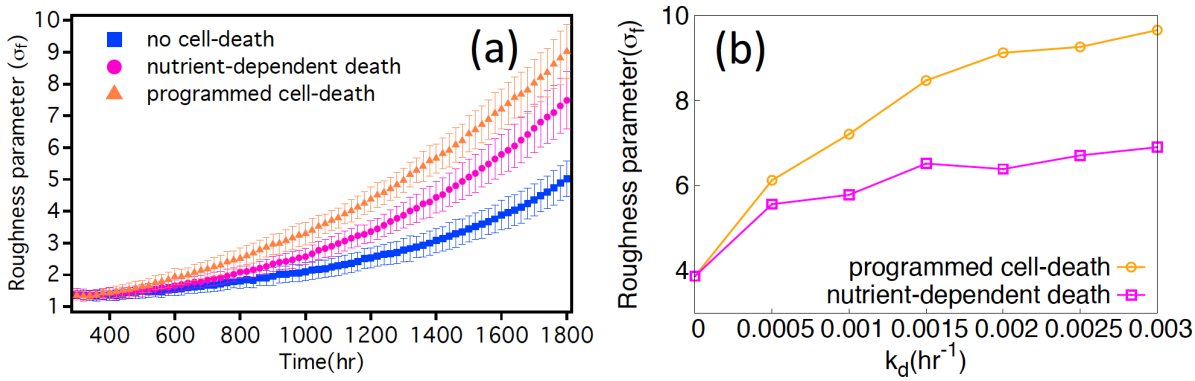

FIG. 4: (Color online) Roughness parameter σ_f, which is determined by calculating the variance in radius of the peripheral bacterial cells of the expanding colonies with respect to time for (A) no death(filled blue squares), nutrient-dependent death(filled magenta circles) and programmed cell-death(filled orange triangles). The cell-death rate is taken as $k_d = 0.001$. (B) Plot of averaged out values of roughness parameter σ_f, from multiple realizations of simulation trajectories as a function of death rate k_d for programmed cell-death (orange curve with empty triangles) and nutrient-dependent cell-death(magenta curve with empty squares). All the other parameters are same as given in the Table-1.

is only slightly reduced in the presence of cell-death. This is directly shown in results for the speed of the colony front in Figure-3B.

It is now necessary to quantify how does cell-death govern the morphology of the growing colony? As we have seen earlier in Figure-2, the colony edge develops more branches as the number of dead cells increases with time. To quantify the effect of cell-death in shaping colony morphology, we determine a roughness parameter(σ_f) characterized by the standard deviation of the distance of the peripheral cells from the center of the box. We plot the time profile of σ_f which is an ensemble average of multiple simulation data as illustrated in Figure-4A for the three different cases: no death, nutrient-dependent death and programmed cell-death. The increase in the value of roughness parameter with respect to time clearly indicates that, in presence of cell-death, bacteria develops highly branched structures at the periphery of the colony. At the same time, we observe that σ_f is higher in case of programmed cell-death as compared to nutrient-dependent death.

We furthermore investigate how does the roughness parameter depend upon the rate of cell-death. In Figure-4B, we plot the ensemble average value of roughness parameter for different values of rate of cell-death k_d after the colony grows for sufficiently long time. We see, that with the increase of rate of cell-death, σ_f monotonically increases up to a certain limit and then saturates to a plateau for higher values of cell-death rate. These observations clearly suggest that cell-death can influence the colony morphology by facilitating transitions from circular to branched structures in multicellular growing systems. For nutrient-limited death, at higher values of cell-death rate k_d, it appears that only the microbial cells

at the colony periphery will grow as a band and the interior will consist entirely of the dead and disintegrated cells. On the other hand, for high apoptotic cell-death rate, the colony becomes very sparse with the presence of dead cells and their removal by disintegration. For very high values of apoptotic cell-death, the whole colony can collapse.

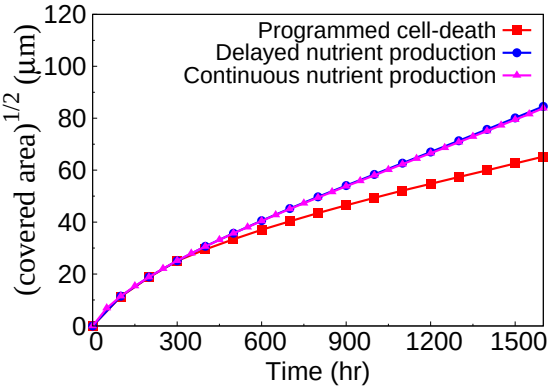

FIG. 5: (Color online) Plot of square root of covered area of the live cells of the expanding colony with respect to time. The red curve with filled squares corresponds to the case of programmed cell-death whereas the blue curve with filled circles and magenta curve with filled triangles (which are basically indistinguishable) correspond to the cases of delayed and continuous production of nutrient by the dead cells during programmed death respectively. For all the three cases, the death rate is taken as $k_d = 0.001$. All the other parameters are the same as given in the Table-1.

We now focus on the possible role of altruism in programmed cell-death. We now assume that dying cells can provide nutrients to the other cells as a way of helping them to overcome nutrient limitation. First, we calculate for the given parameter set, how much nutrient is consumed by an individual bacterial cell as it grows to the maximal threshold length; this equals $12 - 14fg$ for our given parameter set. We presume that nutrient deposition by a dead cell must be less than what it required for growth. Based on these facts, we have chosen an approximate value of nutrient production by the dead cells. We consider two different approaches in order to understand the prospective behavior of the colony in presence of altruistic death. In the first approach we suppose that dead cells during lysis deposit nutrient in the medium continuously until they completely disintegrate with a rate $k_{np} = 3.0$ corresponding to the total deposition of $8fg$ of nutrient per dead cell in the medium. In the second approach, dead cells disintegrate or undergo lysis with a rate $k_{lys} = 1.0$ and after complete disintegration, an amount of metabolite/nutrient is deposited abruptly into the growth medium. Nutrient deposition by dead cells in the local regions allow the remaining neighboring alive cells to utilize the deposited nutrient to grow and survive the nutrient-depletion for longer time. Apparently, there is no significant difference noticeable in the morphology of the spatiotemporal dynamics due to the inclusion of altruism (data not shown). However, if we calculate covered area of the live cells with respect to time for all the three cases: a) cell-death without nutrient production, b) cell-death with continuous nutrient production by dead cells until it completely disintegrate and c) cell-death with delayed nutrient production by dead cells after it completely disintegrate, a significant change can be observed in the number of live bacterial cells, as shown in Figure-5. We found that effective radius which is determined by taking the square root of the covered area of live bacterial cells, is not surprisingly higher in cases of altruistic cell-death compared to non altruistic death, as the released nutrient helps neighboring cells to survive for a longer time.

To better understand the role of mechanical and structural effects of dead cells in regulating colony morphodynamics, we carry out several additional simulations with varied rules. In one of the cases, we allow a dead cell to interact with the same repulsive force as that of live cells as long as it is present in the system. Once it disintegrates there is no longer any repulsive mechanical force. In a second case, the dead cells in the growing colony remain unchanged in their size and shape but have lower elastic repulsive forces ($E_d = 10^4$) of interaction with the neighboring cells. The results of the change of rough-

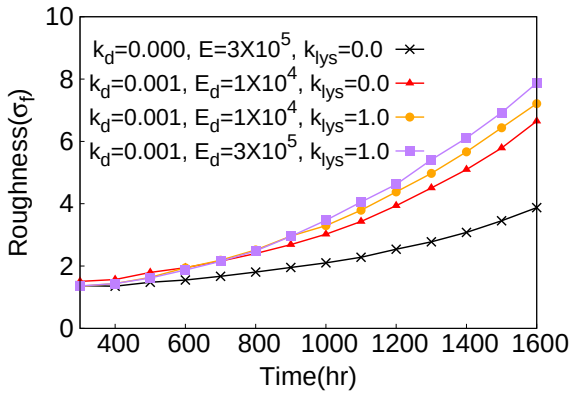

FIG. 6: (Color online) Roughness parameterσ_f of the expanding colonies with respect to the time. The black curve with crosses corresponds to the case of no death ($k_d = 0.0$) in the colony; the red curve with triangles for programmed cell-death ($k_d = 0.001$) with low repulsive coefficients of dead cells ($E_d = 10^4$) without cell-lysis ($k_{lys} = 0.0$) and removal; the orange curve with circles corresponds to the case of programmed cell-death ($k_d = 0.001$) with low elastic repulsive coefficient of dead cell($E_d = 10^4$) and their removal from the system ($k_{lys} = 1.0$); and the purple diamond curve shows the case where dead cells have same repulsive coefficient as alive cells ($E_d = E = 3 \times 10^5$) but undergoes lysis ($k_{lys} = 1.0$) and removal from the growing colony. The rate of cell-death is $k_d = 0.001$ and all the other parameters are kept same as given in the Table-1.

ness parameter σ_f with respect to time for these simulations are compared with the cases of no cell-death in Figure-6. We observe that having weak repulsive forces of dead cells($E_d = 10^4$) without their removal gives rise to lower roughness in the colony fronts than removal of dead cells by disintegration. However, if they are given similar repulsive properties as of the live cells, the dead cells would have a greater impact in creating non-uniformity and sparseness and hence greater roughness in the colony fronts. This appears to be a result of the abrupt loss of strong repulsive forces provided by the dead cells as they vanish from the system. All these observations suggests that the loss of repulsive mechanical forces as a result of disintegration and removal of the dead cells from the growing colony is the key factor which causes a transition from circular to branched structures.

To further investigate how the nutrient depletion pattern and hence associated cell-death is influenced by the initial nutrient concentration C_0, we carried out simulations varying initial nutrient concentration C_0. We find that with higher initial nutrient concentrations, colony size increases as predicted by the total number of live cells demonstrated in Figure-7A. However, interestingly, our simulations reveal that the cells start to die at a later time while growing in lower initial nutrient concentration C_0, for a given threshold concentration C_{thresh} below which cells start to die. In Figure-7B, we plot the temporal evolution of the number of dead cells for three initial nutrient concentrations which shows the onset of cell-death is triggered at much later time for lower C_0s. It turns out from the observation that cell death not only depends upon the local nutrient concentration but also on the local concentration of cells competing for the available nutrient consumption for their growth. In case of lower C_0, the cell growth is slow which also results in a lower local cell-density of bacterial cells compared to that in higher C_0 at a given time. Hence the extent of competition among cells for nutrient consumption is lower at a lower C_0, resulting in a late onset of cell death.

V. CONCLUDING REMARKS

Over the last few decades, there has been a great deal of interest in understanding multicellular organization in bacteria by studying the individual interactions among cells by using agent-based models. The advantage of these models over mean-field level descriptions lies in the fact that they automatically take care of the discrete nature of microbial cells and fluctuations at the interfaces. Cell-death, especially PCD, being one of the important elements of multicellular developmental process, presents both a challenge for basic biological understanding and a potential opportunity for developing effective antibiotic treatment strategies. Although specific mechanisms for cell death in some of these cases have been well characterized [21, 27, 35], the consequences of such a process for a developing multicellular community, such as a biofilm, has been difficult to explore experimentally.

In this article, using an individual-based model, we investigate the role of cell-death in an expanding bacterial colony on semi-solid agar surface. How the interplay of cell-death and mechanical interactions can effectively govern the morphological features of a growing colony is the key result of the present work. We show how either nutrient-limited death and programmed cell-death can significantly influence the growth morphology which is reflected in the spatial behavior by enhanced branch formation at the colony periphery. How the initial nutrient concentration might affect the dynamics is also demonstrated, results which indicates that not only local nutrient concentration but also the local concentration of bacterial cells determines the initiation of cell-death (under the condition of nutrient-dependent cell-death).

It has been established in previous studies [11, 15, 45] that a transition from a circular to branched colony can be driven solely by the uptake of nutrient by bacterial cells and their growth by mechanical pushing; this seems to occur for very slowly moving fronts. However, in our present work, we find that cell-death in a mechanically-driven growing colony will only slightly modifies the effective speed of an expanding colony but it could lead to a significant change in the colony morphology. The underlying reasons appear to be the combined effect of discreteness of cells and inherent fluctuations, a weak repulsive elastic interaction between dead and neighboring cells ,and eventual removal of the dead cells from the system through disintegration which creates void spaces in the colony structure.

Our present model is of course in two dimensions and therefore only sheds direct light on the morphological behavior of a monolayer of bacteria. However, in many cases, bacteria can develop three-dimensional multicellular structures [4, 10, 46]. Extending our work to three dimensions is non-trivial as many new features such as the cell-surface interaction resulting from symmetric or asymmetric adhesion of anisotropic bacteria with the substrate might also influence the structure of a colony [47]. Future studies will indeed aim for such an extension and will explore the role of cell-death along with these complex cell-surface interactions. Nevertheless, our results suggest that also 3D multicellular systems which have highly branched morphology might be strongly influenced by high cell-death during their growth and development.

Acknowledgement: We thank Jagannath Mondal and Prasad Perlekar for careful reading of the manuscript and helpful comments. This work is partially supported by DST-INSPIRE Faculty Award[DST/INSPIRE/04/2015/002495]. This research was also supported by the NSF award (MCB-1241332) and the NSF funded Center for Theoretical Biological Physics (PHY-1427654).

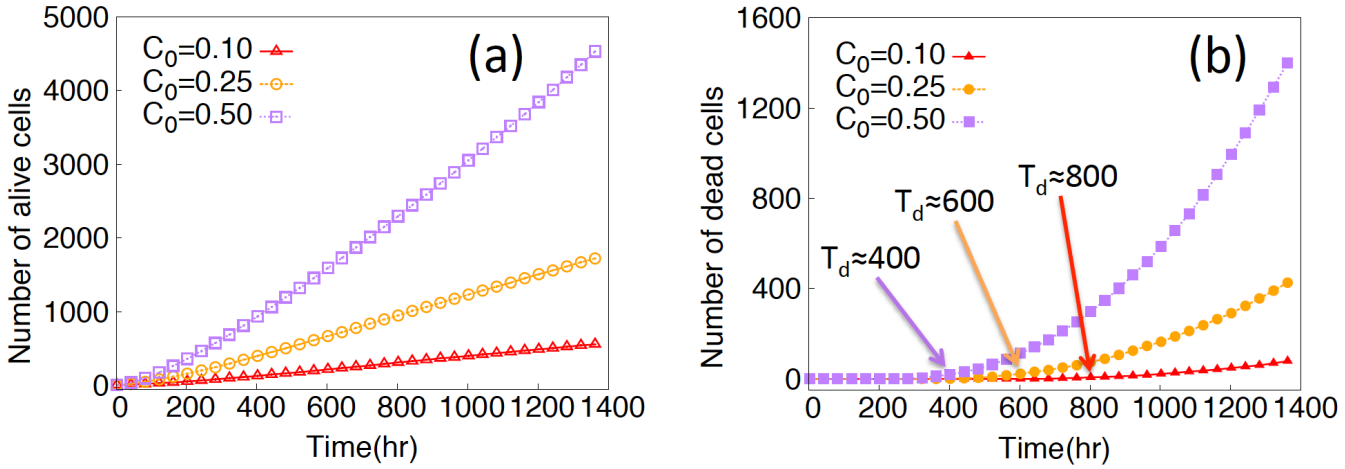

FIG. 7: (Color online) Effect of initial nutrient concentration(C_0) on initiation of cell-death in case of nutrient-dependent death. (A) Plot of total number of alive cells with respect to time for different C_0s. (B) Plot of total number of dead cells with respect to time for different C_0s. The onset of cell-death is represented by T_d. All the other parameters are kept as given in Table-1, in the corresponding simulations.

[1] G. A. O'Toole and R. Kolter, Mol. Microbiol. **30**, 295 (1998).
[2] K. W. Bayles, Nat. Rev. Micro. **5**, 721 (2007).
[3] J. W. Costerton, Z. Lewandowski, D. E. Caldwell, D. R. Korber, and H. M. Lappin-Scott, Annu. Rev. Microbiol. **49**, 711 (1995).
[4] M. Asally, M. Kittisopikul, P. Ru, Y. Du, Z. Hu, T. aatay, A. B. Robinson, H. Lu, J. Garcia-Ojalvo, and G. M. Sel, Proc. Natl. Acad. Sci. U.S.A. **109**, 18891 (2012).
[5] A. Be'er, H. P. Zhang, E.-L. Florin, S. M. Payne, E. Ben-Jacob, and H. L. Swinney, Proc. Natl. Acad. Sci. U.S.A. **106**, 428 (2009).
[6] E. Ben-Jacob, I. Cohen, and H. Levine, Adv. Phys. **49**, 395 (2000).
[7] H. Cho, H. Jansson, K. Campbell, P. Melke, J. W. Williams, B. Jedynak, A. M. Stevens, A. Groisman, and A. Levchenko, PLoS Biol. **5**, e302 (2007).
[8] D. Volfson, S. Cookson, J. Hasty, and L. S. Tsimring, Proc. Natl. Acad. Sci. U.S.A. **105**, 15346 (2008).
[9] H. P. Zhang, A. Beer, E.-L. Florin, and H. L. Swinney, Proc. Natl. Acad. Sci. U.S.A. **107**, 13626 (2010).
[10] D. Boyer, W. Mather, O. Mondragn-Palomino, S. Orozco-Fuentes, T. Danino, J. Hasty, and L. S. Tsimring, Phys. Biol. **8**, 026008 (2011).
[11] F. D. C. Farrell, O. Hallatschek, D. Marenduzzo, and B. Waclaw, Phys. Rev. Lett. **111**, 168101 (2013).
[12] M. C. Marchetti, J. F. Joanny, S. Ramaswamy, T. B. Liverpool, J. Prost, M. Rao, and R. A. Simha, Rev. Mod. Phys. **85**, 1143 (2013).
[13] R. Balagam and O. A. Igoshin, PLoS Comput. Biol. **11**, 1 (2015).
[14] P. Ghosh, E. Ben-Jacob, and H. Levine, Phys. Biol. **10**, 066006 (2013).
[15] P. Ghosh, J. Mondal, E. Ben-Jacob, and H. Levine, Proc. Natl. Acad. Sci. U.S.A. **112**, E2166 (2015).
[16] C. M. Waters and B. L. Bassler, Annu. Rev. Cell Dev. Biol. **21**, 319 (2005).
[17] X. Fu, L.-H. Tang, C. Liu, J.-D. Huang, T. Hwa, and P. Lenz, Phys. Rev. Lett. **108**, 198102 (2012).
[18] S. Payne, B. Li, Y. Cao, D. Schaeffer, M. D. Ryser, and L. You, Mol. Syst. Biol. **9** (2013).
[19] B. Liebchen, D. Marenduzzo, I. Pagonabarraga, and M. E. Cates, Phys. Rev. Lett. **115**, 258301 (2015).
[20] J. S. Webb, L. S. Thompson, S. James, T. Charlton, T. Tolker-Nielsen, B. Koch, M. Givskov, and S. Kjelleberg, J. Bacteriol. **185**, 4585 (2003).
[21] Y. Tanouchi, A. Pai, N. E. Buchler, and L. You, Mol. Syst. Biol. **8**, 1744 (2012).
[22] N. Allocati, M. Masulli, C. Di Ilio, and V. De Laurenzi, Cell Death Dis. **6**, e1609 (2015).
[23] D. J. Dwyer, D. M. Camacho, M. A. Kohanski, J. M. Callura, and J. J. Collins, Mol. Cell **46**, 561 (2012).
[24] J. S. Webb, M. Givskov, and S. Kjelleberg, Curr. Opin. Microbiol. **6**, 578 (2003).
[25] P. Meier, A. Finch, and G. Evan, Nature **407**, 796 (2000).
[26] H. Engelberg-Kulka, S. Amitai, I. Kolodkin-Gal, and R. Hazan, PLoS Genet. **2**, e135 (2006).
[27] A. Erental, I. Sharon, and H. Engelberg-Kulka, PLoS Biol. **10**, e1001281 (2012).
[28] M. G. Fagerlind, J. S. Webb, N. Barraud, D. McDougald, A. Jansson, P. Nilsson, M. Harln, S. Kjelleberg, and S. A. Rice, J. Theor. Biol. **295**, 23 (2012).
[29] J. E. Gonzlez-Pastor, E. C. Hobbs, and R. Losick, Science **301**, 510 (2003).
[30] I. S. Tan, C. A. Weiss, D. L. Popham, and K. S. Ramamurthi, Dev. Cell **34**, 682 (2015).
[31] D. Claessen, D. E. Rozen, O. P. Kuipers, L. Sogaard-Andersen, and G. P. van Wezel, Nat. Rev. Micro. **12**, 115 (2014).
[32] K. Lewis, Microbiol. Mol. Biol. Rev. **64**, 503 (2000).
[33] K. W. Bayles, Nat. Rev. Micro. **12**, 63 (2014).
[34] J. W. Wireman and M. Dworkin, J. Bacteriol. **129**, 798

(1977).
[35] H. R. Meredith, J. K. Srimani, A. J. Lee, A. J. Lopatkin, and L. You, Nat. Chem. Biol. **11**, 182 (2015).
[36] C.-F. C and X. JB, Mol. Syst. Biol. **8**, 627 (2012).
[37] E. S. Gloag, L. Turnbull, A. Huang, P. Vallotton, H. Wang, L. M. Nolan, L. Mililli, C. Hunt, J. Lu, S. R. Osvath, et al., Proc. Natl. Acad. Sci. U.S.A. **110**, 11541 (2013).
[38] M. Allesen-Holm, K. B. Barken, L. Yang, M. Klausen, J. S. Webb, S. Kjelleberg, S. Molin, M. Givskov, and T. Tolker-Nielsen, Mol. Microbiol. **59**, 1114 (2006).
[39] M. Matsushita, F. Hiramatsu, N. Kobayashi, T. Ozawa, Y. Yamazaki, and T. Matsuyama, Biofilms **1**, 305 (2004), ISSN 1479-0513.
[40] J. A. Bonachela, C. D. Nadell, J. B. Xavier, and S. A. Levin, J. Stat. Phys. **144**, 303 (2011).
[41] D. A. Kessler and H. Levine, Nature **394**, 556 (1998).
[42] S. Arouh and H. Levine, Phys. Rev. E **62**, 1444 (2000).
[43] I. Golding, Y. Kozlovsky, I. Cohen, and E. Ben-Jacob, Physica A: Statistical Mechanics and its Applications **260**, 510 (1998).
[44] M. Godin, F. F. Delgado, S. Son, W. H. Grover, A. K. Bryan, A. Tzur, P. Jorgensen, K. Payer, A. D. Grossman, M. W. Kirschner, et al., Nat. Meth. **7**, 387 (2010).
[45] C. Giverso, M. Verani, and P. Ciarletta, J. R. Soc. Interface **12**, 20141290 (2015).
[46] J. Yan, A. G. Sharo, H. A. Stone, N. S. Wingreen, and B. L. Bassler, Proc. Natl. Acad. Sci. U.S.A. **113**, E5337 (2016).
[47] M.-C. Duvernoy, T. Mora, M. Ardre, V. Croquette, D. Bensimon, C. Quilliet, J.-M. Ghigo, M. Balland, C. Beloin, S. Lecuyer, et al., bioRxiv. (2017), URL `http://www.biorxiv.org/content/early/2017/01/31/104679`.